Journal of Sound and Vibration 327 (2009) 163–172

Contents lists available at ScienceDirect

Journal of Sound and Vibration

journal homepage: www.elsevier.com/locate/jsvi

The Westervelt equation with viscous attenuation versus a causal propagation operator: A numerical comparison

Guy V. Norton *, Robert D. Purrington

Tulane University, New Orleans, LA, USA

ARTICLE INFO

Article history:
Received 12 February 2009
Received in revised form
19 May 2009
Accepted 28 May 2009
Handling Editor: C.L. Morfey
Available online 9 July 2009

ABSTRACT

The numerical solution of acoustic pulse propagation through dispersive media requires the inclusion of attenuation and its causal companion, phase velocity. For the case of propagation in a linear medium, Szabo [Time domain wave equations for lossy media obeying a frequency power law, *Journal of the Acoustic Society of America* 96 (1994) 491–500] introduced the concept of a causal convolutional propagation operator that plays the role of a causal propagation factor in the time domain. The convolutional operator has been successfully employed in the linear wave equation for both isotropic and non-isotropic dispersive media. This operator was originally proposed by Szabo to replace the loss term responsible for attenuation due to thermal conduction and viscosity of the fluid in the Westervelt equation. The Westervelt equation with a traditional loss term fails to incorporate the full dispersive characteristics of the medium, a deficiency which can be removed, at least in principle by replacing the traditional loss term with the causal convolutional propagation factor. Previously no comparison has been made between the Westervelt equation with the traditional loss term and with Szabo's causal convolutional propagation operator. In this paper we show numerically that by employing the convolutional propagation operator the full dispersive characteristics of the media are properly incorporated into the solution, and that the results can differ significantly from the Westervelt equation with the traditional loss term. The equations will be solved via the method of finite differences.

1. Introduction

When the medium in which acoustic energy is being propagated is dispersive, causality requires that the propagating field will be attenuated, and that attenuation will be frequency-dependent. If the source is time limited, i.e. an acoustic pulse, its frequency content will be appropriately broad, and to accurately treat such a situation the model will have to be able to take into account this frequency-dependence of the attenuation and phase velocity for the spread of frequencies contributing to the source. In this case, modeling in the time domain (rather than the frequency domain) is highly desirable, since it allows for more direct and efficient numerical solution of the appropriate wave equation, and causality is always fulfilled.

Based on an idea set forth by Blackstock [1] in the context of nonlinear acoustics, Szabo offered a way to include attenuation and dispersion effects directly in the time domain for both nonlinear [2] and linear propagation [3–5] in linear media, through the introduction of a causal convolutional propagation operator into the corresponding three-dimensional

* Corresponding author.
E-mail address: gnorton@tulane.edu (G.V. Norton).

0022-460X/$ - see front matter © 2009 Elsevier Ltd. All rights reserved.
doi:10.1016/j.jsv.2009.05.031

wave equation. By deriving a time domain version [3] of the Kramers–Krönig relations (K–K) [6], he arrived at a general form for the propagation operator. Szabo's operator was originally defined in the context of lossy media obeying a frequency power law attenuation, but Waters et al. [7] showed that Szabo's approach could be extended to a broader class of media (as originally suggested by Blackstock), provided the attenuation possesses a Fourier transform in a distributional sense.

Norton and Novarini [8] clarified the use of the causal convolutional propagation operator and its relationship to the *time domain propagation factor* (TDPF) (see Section 3). The time domain propagation factor is directly related to the dispersive properties (attenuation and dispersion) of the medium. The modified wave equation containing the causal convolutional propagation operator is rewritten incorporating the time domain propagation factor explicitly. The capability of the time domain propagation factor to correctly incorporate the dispersive traits of the medium into the linear wave equation was demonstrated by solving the one-dimensional scalar, inhomogeneous wave equation in a dispersive medium via a finite-difference-time-domain scheme [8]. Thus, if the frequency-dependence of the attenuation is known, either from measurement or theoretically and if it possesses a generalized Fourier transform, then the time domain propagation factor, and hence the corresponding causal convolutional propagation operator, can be obtained. Given the propagation operator, causal propagation can be modeled directly in the time domain.

Norton and Novarini [9] extended the technique to 2-D non-isotropic media, in which the dispersive effects vary spatially. Excellent agreement between the FDTD with dispersion and the analytic result was observed for both the forward and the backscattered field. Enhancements to the numerical scheme included making all difference approximations of the derivatives (both space and time) fourth-order accurate as well as making the absorbing boundary conditions, utilizing the complementary operator method (COM) fourth-order accurate [10]. Norton and Novarini [11] have utilized this model to investigate the scattering from and propagation through bubble clouds in the ocean. Norton and Novarini [12] have also applied this technique to scattering and propagation in biological tissue, examining the impact that dispersion has on the backscattered signal. The target media studied consisted of brain, heart, kidney, liver and tendon tissue. Finally Norton [13,14] extended the technique to include heterogeneous dispersive media, recasting the modified wave equation so that it had a spatially varying bulk modulus and density.

Previous use of the causal time domain propagation factor has been limited to the linear wave equation. In this paper we apply this term to the Westervelt equation, which permits realistic inclusion of attenuation (and its causal companion, phase velocity) and nonlinear effects. Traditionally, when the medium is taken to be a thermoviscous fluid, the Westervelt equation with a traditional loss term is employed. To this point no comparison has been made between employing the Westervelt equation with the traditional loss term (Eq. (2)) and that utilizing Szabo's causal time domain propagation factor. This paper makes this comparison, numerically, by modeling acoustic propagation with the Westervelt equation including the causal time domain propagation factor. We will show that this correctly incorporates the full dispersive characteristics of the medium. Specifically we show that employing the causal time domain propagation factor can produce results that differ significantly from employing the Westervelt equation with the traditional loss mechanism, which is due to the fact that the latter fails to take into account the full dispersive characteristics of the medium.

We begin by incorporating dispersive effects into the Westervelt equation for sound propagation in a fluid medium through the inclusion of the causal time domain propagation factor. The finite-difference formalism is then described, and a numerical experiment is carried out in one dimension, using the two forms of the Westervelt equation given in Eqs. (2) and (6), below, that is, with and without the time domain propagation factor. Finally the differences and similarities between the two approaches are discussed and compared with an analytical solution.

2. Westervelt equation for non-dispersive and dispersive media

The Westervelt equation describing the propagation of finite amplitude sound has the following form [15]:

$$\nabla^2 p - \frac{1}{c_0^2}\frac{\partial^2 p}{\partial t^2} + \frac{\beta}{\rho_0 c_0^4}\frac{\partial^2 p^2}{\partial t^2} = 0, \tag{1}$$

where p is the acoustic pressure, ρ_0 and c_0 are the ambient density and sound speed, $\beta = 1 + (B/2A)$ is the nonlinearity coefficient for the fluid, and B/A is the nonlinearity parameter. The first two terms in Eq. (1), the D'Alembertian operator acting on the acoustic pressure, describe linear lossless wave propagation at the small-signal sound speed. The final term describes nonlinear distortion of the wave due to finite-amplitude effects.

If the medium is assumed to be a thermoviscous fluid, the Westervelt equation (Eq. (1)) takes the following form [16]:

$$\nabla^2 p - \frac{1}{c_0^2}\frac{\partial^2 p}{\partial t^2} + \frac{\delta}{c_0^4}\frac{\partial^3 p}{\partial t^3} + \frac{\beta}{\rho_0 c_0^4}\frac{\partial^2 p^2}{\partial t^2} = 0. \tag{2}$$

The additional term is a loss term, which is due to the thermal conduction and the viscosity of the fluid. Here δ is the diffusivity of sound; in a thermoviscous fluid, the absorption coefficient α is related to δ and $\omega = 2\pi f$ by

$$\delta = \frac{2c_0^3\alpha}{\omega^2}. \tag{3}$$

The absorption coefficient is a constant, specific to a single frequency. In the next section we introduce the causal time domain propagation factor, which incorporates a frequency-dependent attenuation and phase velocity.

3. The causal time domain propagation factor

A brief review of the development of the time domain propagation factor is as follows (see Refs. [4,8] for details). Assuming that propagation takes place in a lossy linear medium, the propagation can be shown to be governed by a modified form of Eq. (1). The modification consists of including a causal convolutional propagation operator ($L_\gamma(t)$) which controls attenuation and dispersion. It plays the role of a generalized dissipative term in the time domain. The Westerfelt equation then takes the form

$$\nabla^2 p - \frac{1}{c_0^2}\frac{\partial^2 p}{\partial t^2} + \frac{1}{c_0}(L_\gamma(t) * p) + \frac{\beta}{\rho_0 c_0^4}\frac{\partial^2 p^2}{\partial t^2} = 0, \tag{4}$$

where $*$ represents a convolution.

In the framework of generalized functions, assuming that the pressure field is a distribution and recalling that distributional differentiation is equivalent to a convolution with a derivative of the Dirac delta function $[\delta^{(1)}(t) * f(t) = f^{(1)}(t)]$, the operator can be defined as

$$L_\gamma(t) \equiv \Gamma(t) * \delta^{(1)}(t). \tag{5}$$

The function $\Gamma(t)$ represents the causal time domain propagation *factor* that accounts for causal attenuation, that is, it governs dispersion in the system to insure causality. Eq. (4) can now be written in terms of $\Gamma(t)$ as

$$\nabla^2 p - \frac{1}{c_0^2}\frac{\partial^2 p}{\partial t^2} + \frac{1}{c_0}\frac{\partial[\Gamma(t) * p]}{\partial t} + \frac{\beta}{\rho_0 c_0^4}\frac{\partial^2 p^2}{\partial t^2} = 0. \tag{6}$$

Note that it is the time domain propagation factor $\Gamma(t)$ that is required and not ($L_\gamma(t)$).

In the frequency domain, propagation in a dispersive medium can be described through a complex propagation factor

$$k(\omega) = -\alpha(\omega) + \mathrm{i}\beta(\omega), \tag{7}$$

where $\alpha(\omega)$ is the frequency-dependent attenuation and $\beta(\omega) = (\omega/c_0) + \beta'(\omega)$ is the real wavenumber, with $\beta'(\omega)$, its dispersive component, given by

$$\beta'(\omega) = \omega\left[\frac{1}{c(\omega)} - \frac{1}{c_0}\right]. \tag{8}$$

The complex propagation factor can also be expressed as

$$k(\omega) = \gamma'(\omega) + \mathrm{i}\frac{\omega}{c_0}. \tag{9}$$

Here $\gamma'(\omega) = -\alpha(\omega) + \mathrm{i}\beta'(\omega)$ represents the dispersive component of the complex propagation factor. Szabo [3] defined the causal time domain propagation factor as the inverse Fourier transform of $\gamma'(\omega)$

$$\Gamma(\tau) = FT^{-1}\{\gamma'(\omega)\}, \tag{10}$$

where τ is the retarded time $\tau = (t-r)/c_0$. Since in a weakly dispersive media $\alpha(\omega)$ and $\beta'(\omega)$ are related by causality through the (K–K) relations (they are the Hilbert transform of each other), then

$$\beta'(\omega) = -H\{-\alpha(\omega)\}. \tag{11}$$

This leads to

$$\Gamma(\tau) = -2 1_+(\tau) FT^{-1}\{\alpha(\omega)\}, \tag{12}$$

where $1_+(\tau)$ represents the step function defined as [17]

$$1_+ \equiv \begin{cases} 0 & \tau < 0, \\ \frac{1}{2} & \tau = 0, \\ 1 & \tau > 0. \end{cases} \tag{13}$$

Szabo originally limited the use of the time domain propagation operator to a power law attenuation, and excluding some values of the exponent, as already noted. Waters et al. [7], using distributional analysis, showed that Eq. (12) is more general and can be applied to any attenuation form for which an associated causal phase velocity exists.

4. Finite difference formulation

A one-dimensional numerical solution of Eqs. (2) and (6) was performed using a FDTD representation of Eqs. (2) and (6) that was explicitly fourth order in both time and space. The second partial of the pressure with respect to time was extended to fourth order. However, because the usual fourth-order finite difference representation of the second partial derivative would lead to an unconditionally unstable scheme, a technique given by Cohen [18] based on the "modified equation approach" to obtain fourth-order accuracy in time was used. This technique, while improving the accuracy in time, preserves the simplicity of the second-order accurate time-step scheme. This was performed in order that all derivatives have the same order of accuracy as the boundary conditions which are also fourth order. It was found [10] that lower order boundary conditions did not suppress spurious reflections at the computational boundary that could contaminate low amplitude signals (i.e. backscattered signals) of interest. The reader is directed to Ref. [10] for further information and explanation. The temporal derivatives were calculated as follows:

$$\frac{\partial p}{\partial t} = \frac{1}{12\Delta t}(25p_i^n - 48p_i^{n-1} + 36p_i^{n-2} - 16p_i^{n-3} + 3p_i^{n-4}),$$

$$\frac{\partial^2 p}{\partial t^2} = \frac{p_i^{n+1} - 2p_i^n + p_i^{n-1}}{\Delta t^2} - \frac{c^4\Delta t^2}{12\Delta x^4}(6p_i^n - 4(p_{i+1}^n + p_{i-1}^n) + p_{i+2}^n + p_{i-2}^n),$$

$$\frac{\partial^3 p}{\partial t^3} = \frac{1}{2\Delta t^3}(6p_i^n - 23p_i^{n-1} + 34p_i^{n-2} - 24p_i^{n-3} + 8p_i^{n-4} - p_i^{n-5}). \tag{14}$$

The first derivative term is associated with the nonlinearity and the third derivative term is the loss term.

The spatial differences were computed using a fourth-order accurate centered differencing scheme

$$\frac{\partial^2 p}{\partial x^2} = \frac{1}{12\Delta x^2}(-p_{i+2}^n + 16p_{i+1}^n - 30p_i^n + 16p_{i-1}^n - p_{i-2}^n). \tag{15}$$

A technique known as the complementary operator method was utilized [19] in the development of the absorbing boundary conditions (ABC). The details of the derivation of the COM operators are beyond the scope of this paper; the interested reader should refer to Ref. [19]. This technique was first utilized in electromagnetics where it was shown to yield excellent results [19]. The COM method is a differential equation-based ABC method, and differs from the other common approach of terminating the grid with the use of an absorbing material. An example of this type of boundary condition is the perfectly matched layer (PML) method originally proposed by Berenger [20]. The COM requires the summation of two simulations. The first simulation results from using an ABC that operates on the field in a known manner. The second simulation is performed using the complement of the ABC. The energy reflected by this complementary ABC has the same amplitude as the original ABC but is opposite in phase. Thus when the two simulations are averaged the resulting solution is nearly free of all the energy introduced by the ABC. The COM is based on one-way wave equations such as Higdon's boundary operators [21].

5. Numerical experiment

The numerical experiment is carried out in one dimension. The input signal is a 1 MHz sinusoidal burst of six cycles modulated by a Gaussian envelope in time. The numerical grid consists of 1500 points with $\Delta X = 0.1$ mm. The time increment is $\Delta t = 10.681$ ns. The source is located at $X = 3.5$ cm. The first receiver is located at $X = 5$ cm and the second is located at $X = 7$ cm. The medium simulated is mammalian liver tissue in which the non-dispersive sound speed is $1600\,\mathrm{m\,s^{-1}}$ and the density of the tissue is taken to be $1100\,\mathrm{kg\,m^{-3}}$. The attenuation is assumed to have a power law dependence

$$\alpha(\omega) = \alpha_0\omega^y = (2.0976\times10^{-7}\,\mathrm{Np\,m^{-1}\,rad^{-1}\,s^{-1}})\omega^{1.13}. \tag{16}$$

Fig. 1 displays the attenuation in $\mathrm{dB\,m^{-1}}$ versus frequency. The causal phase velocity that is associated with this attenuation is shown in Fig. 2. The truncated source, which is a sinusoid of constant frequency but finite time duration, has a significant frequency content, as shown in Fig. 3, which depicts the frequency spectrum of the source. The source has a bandwidth of approximately 1 MHz with a center frequency of 1 MHz. The use of the time domain propagation factor in Eq. (6) results in each frequency associated with the source having a different attenuation and phase velocity (see Figs. 1 and 2). When solving Eq. (2), however, the attenuation associated with the peak frequency (1 MHz) (see Eq. (3)) is used, that is, $87.5\,\mathrm{dB\,m^{-1}}$ or approximately $10.1\,\mathrm{Np\,m^{-1}}$. In solving Eq. (6), a maximum of 1000 points is used for the convolution.

Numerical results from the FDTD solutions to Eqs. (2) and (6) at two receiver locations are Fourier transformed into the frequency domain allowing for the determination of the frequency-dependence of the attenuation and phase velocity, which are obtained from the following expressions:

$$\alpha(f) = \frac{8.68\left(\frac{p(x_2,f)}{p(x_1,f)}\right)}{d}, \tag{17}$$

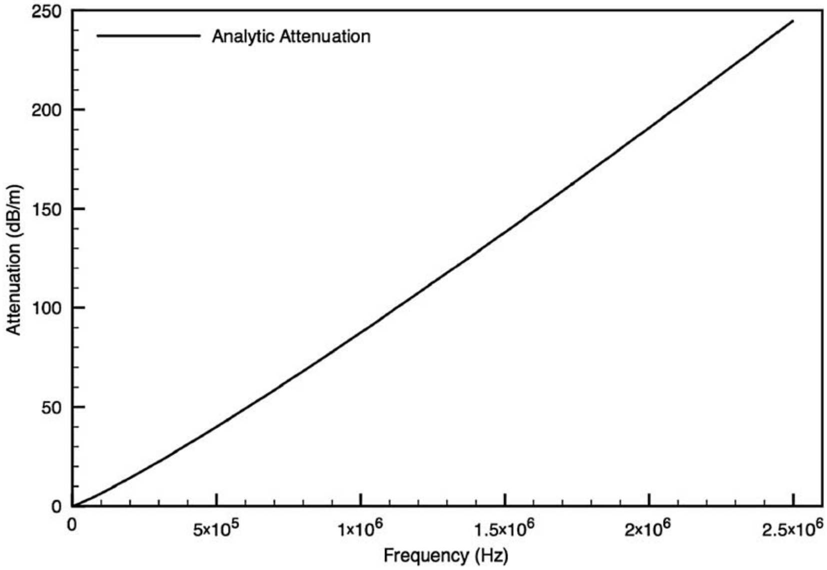

Fig. 1. Attenuation versus frequency.

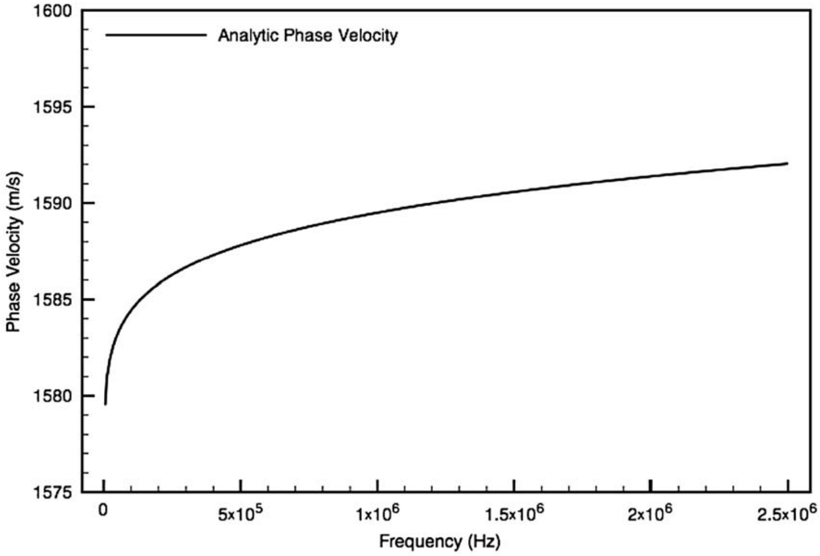

Fig. 2. Phase velocity versus frequency.

$$c(f) = \frac{2\pi f d}{\mathrm{ARG}(p(x_2,f)/p(x_1,f))}, \tag{18}$$

where d is the distance in meters separating the two receivers.

In order to compare the effect that the two loss terms have on the propagating signal, the effects of nonlinearity are removed by setting $p_0 = 1\,\mathrm{Pa}$. This permits highlighting the effect of each loss term. Utilizing Eqs. (17) and (18), the attenuation and phase velocity can be extracted for each case and compared to the analytic solution. Fig. 4 compares the analytic attenuation (from Fig. 1; solid line) to the attenuation extracted from the solution of Eq. (2) (dotted line) and of Eq. (6) (dashed line). The range of frequencies corresponds to the frequency content of the source (see Fig. 3). The extracted attenuation from Eq. (6), utilizing the time domain propagation factor, is essentially indistinguishable from the analytic attenuation, indicating that the time domain propagation factor is introducing the correct amount of loss at each frequency. The attenuation as a function of frequency based on Eq. (2) crosses the analytic curve at the center frequency of 1 MHz. At frequencies below the peak frequency, the viscous term produces less attenuation than the causal operator, with the situation reversed above the peak frequency. There is a frequency squared dependence on attenuation as one would expect (see Eq. (3)), and indeed for any medium Eq. (2) imposes a frequency squared dependence on the attenuation.

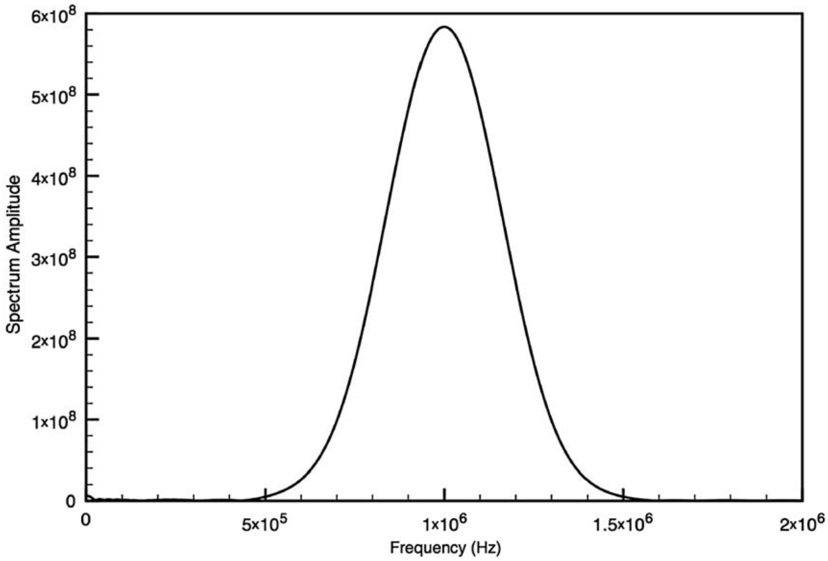

Fig. 3. Frequency spectrum of source.

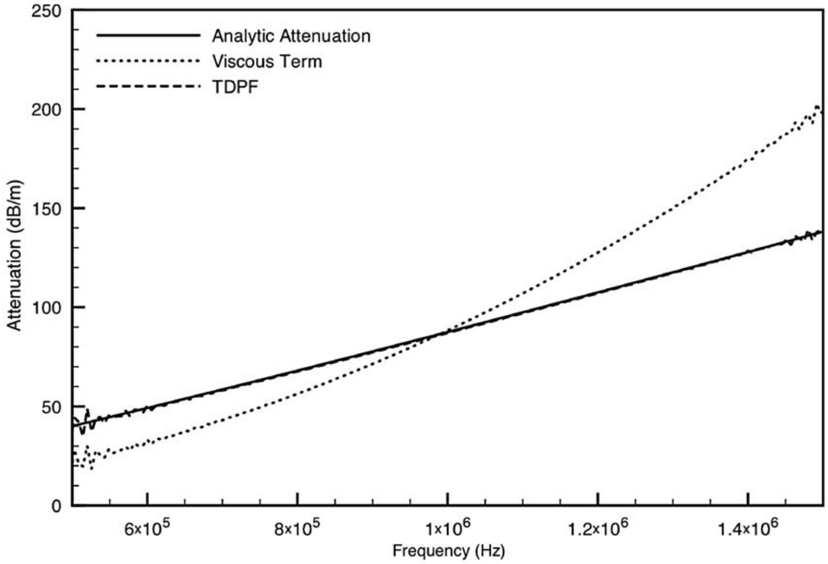

Fig. 4. Comparison of extracted to analytic attenuation.

Fig. 5 compares the phase velocity associated with the analytic attenuation to that extracted from the propagated signals using Eqs. (2) and (6). The phase velocity extracted using the time domain propagation factor (Eq. (6)) again agrees very well with the analytic values. It is worth emphasizing that while the value of c_0 used in both Eqs. (2) and (6) is $1600.0\,\mathrm{m\,s^{-1}}$, the time domain propagation factor associates the proper phase velocity with each frequency automatically, but in the time domain. The phase velocity extracted using Eq. (2), the dotted line in Fig. 5, is the same at all frequencies, since there is no dispersion in this case.

Fig. 6 compares the time series at the second receiver ($X = 7\,\mathrm{cm}$), showing that the signal propagated via Eq. (6) suffers from dispersion (arrives later and has spread out in time) while the signal associated with Eq. (2) does not.

In order to investigate the effects of nonlinearity along with attenuation, the source pressure amplitude p_0 is now set to 5.0 MPa. The nonlinear term (final term) in Eqs. (2) and (6) now has an impact on the propagated field. Fig. 7 compares the time series for three cases: first, with no attenuation (solid line); second, when the viscous term (Eq. (2)) is used (dotted line); and lastly using Eq. (6), with the time domain propagation factor (dashed line). Comparing Figs. 7 to 6 the effects of the nonlinear term are easily observed. The time series for the zero attenuation case shows a steepening of the signal as well as several turning points, not observed in Fig. 6. When attenuation is included, whether from the viscous term or from

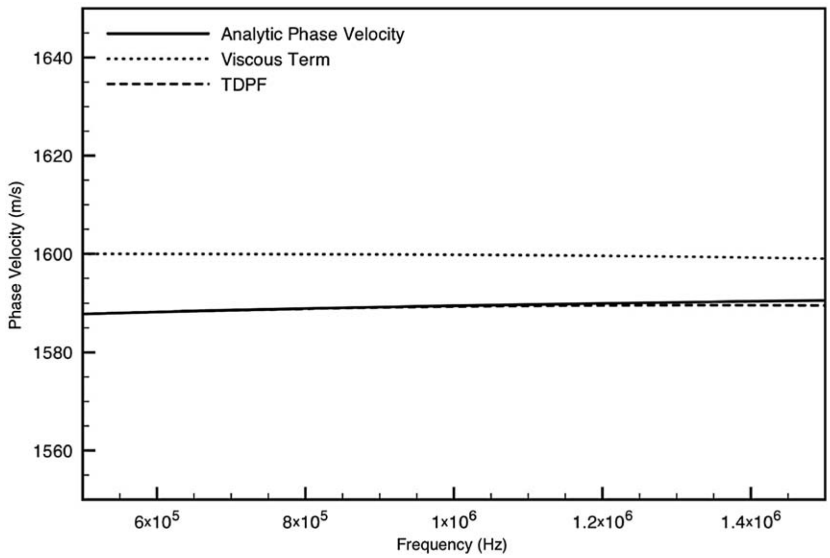

Fig. 5. Comparison of extracted to analytic phase velocity.

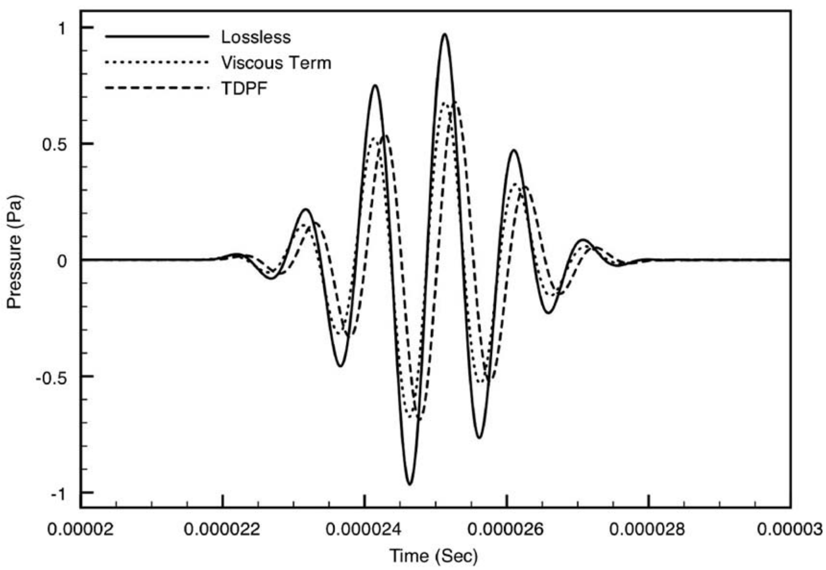

Fig. 6. Comparison of time series.

the time domain propagation factor, these turning points are smoothed and the overall signal amplitude is reduced. The smoothing is greater with the viscous term (Eq. (2)) than when using the time domain propagation factor (Eq. (6)). The dispersive characteristic of the time series using the time domain propagation factor is clearly observed.

Fig. 8 compares the signal spectrum at the second receiver. Note that in this nonlinear case, the unattenuated signal now has energy in the first two harmonics of the original signal (2 and 3 MHz). When attenuation is included, the amplitude at the source frequency is reduced as are the amplitudes of the two harmonics. While the signal amplitudes are nearly the same at the source frequency for the two attenuation cases, their amplitudes at the two harmonics are not. The result using the time domain propagation factor forces more energy into the two harmonics than when using the viscous term.

To further investigate the effects of the different attenuation terms, the following comparisons are made. The acoustic field using the two different loss terms is integrated over time at both receiver locations ($X = 5$ and 7 cm). These values are now compared to the integrated value for the lossless case, with the results for the signal loss (SL) expressed in dB

$$\mathrm{SL(dB)} = 10\,\log\left(\frac{\int(p_{\mathrm{lossterm}}(x_{\mathrm{rec}},t)\times p_{\mathrm{lossterm}}(x_{\mathrm{rec}},t))\,\mathrm{d}t}{\int(p_{\mathrm{noloss}}(x_{\mathrm{rec}},t)\times p_{\mathrm{noloss}}(x_{\mathrm{rec}},t))\,\mathrm{d}t}\right). \tag{19}$$

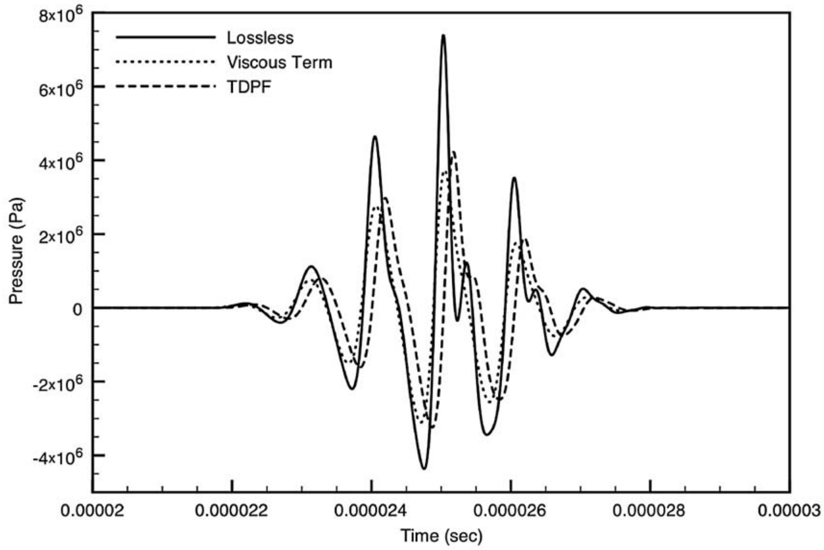

Fig. 7. Nonlinear time series.

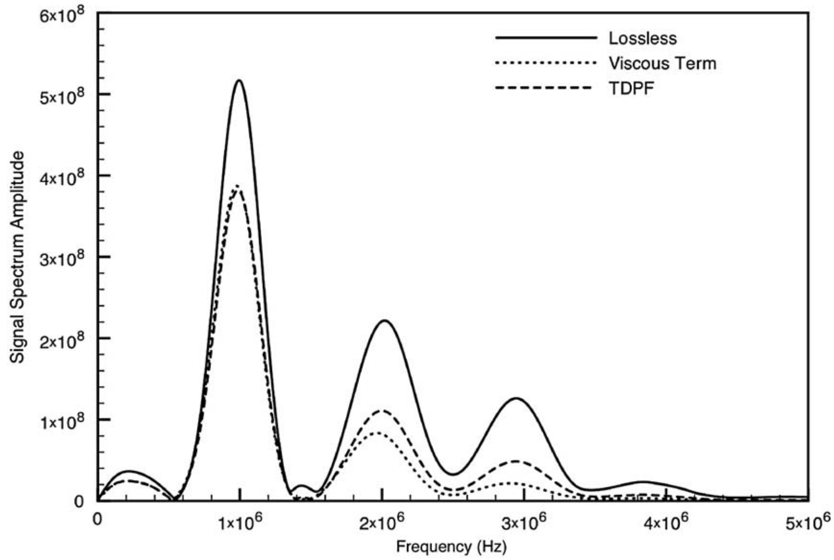

Fig. 8. Signal spectrum.

This loss (SL) is compared to the analytic value, using the attenuation at 1 MHz and the distance from the source location to each receiver. The signal loss at each receiver is

$$\mathrm{SL}_1 = 87.5\,\mathrm{dB\,m^{-1}} \times 0.015\,\mathrm{m} = 1.31\,\mathrm{dB},$$

$$\mathrm{SL}_2 = 87.5\,\mathrm{dB\,m^{-1}} \times 0.035\,\mathrm{m} = 3.06\,\mathrm{dB}. \tag{20}$$

Table 1, below, compares the losses for three different values of p_0. The linear case is represented by $p_0 = 1$ Pa. The amount of signal loss using either loss term results in a good agreement with the analytic expression. However, when p_0 is increased so that the nonlinear term becomes important, the two techniques begin to differ.

The approximate location of shock formation can be determined from the following expression [22]:

$$\bar{x} = \frac{\rho c^2}{\beta k p_0}. \tag{21}$$

Table 1
Signal loss at second receiver for various values of p_0.

p_0	Viscous term (dB)	Causal operator (dB)
1 Pa	3.08	3.03
5 MPa	3.45	3.28
10 MPa	4.47	3.97

Table 2
Signal loss at first receiver for various values of p_0.

p_0 (MPa)	Viscous term (dB)	Causal operator (dB)
5	1.39	1.32
10	1.6	1.44

For $p_0 = 5$ MPa the location of shock formation is 6.1 cm, and for $p_0 = 10$ MPa it is at 4.8 cm. Consequently, when $p_0 = 10$ MPa, shock formation begins before the signal arrives at either receiver location. This may account for the increase in the losses seen in Table 1. Table 2 displays the losses determined from Eq. (14) at the first receiver location, $X = 5$ cm.

One sees that the approximate location of shock formation when $p_0 = 5$ MPa is beyond the first receiver, and in this case as can be seen from Table 2, losses deriving from either loss term are close to the analytic value. On the other hand, when $p_0 = 10$ MPa shock formation occurs before the first receiver and the losses determined by either loss term exceeds the analytic value, with the losses determined due to the viscous term (Eq. (2)) exceeding that due to the use of the time domain propagation factor (Eq. (6)).

6. Concluding remarks

Two variations of the Westervelt equation including attenuation were solved using the method of finite differences. In the first (viscous) case, the attenuative term employed the third time derivative of the pressure, while the second case utilized a time domain propagation factor that introduces both attenuation and dispersive effects into the solution. It has been shown that the time domain propagation factor imparts the correct phase velocity and attenuation to the signal. When the nonlinear term influences the signal, the attenuation terms tend to diminish the nonlinear affect. The energy that is pumped into the higher harmonics of the source differs depending on whether the viscous term or the time domain propagation factor is used, with the time domain propagation factor putting more energy in the higher harmonics than the viscous term. This work was performed as a proof of concept for utilizing the time domain propagation factor in a nonlinear equation to numerically take into account the dispersive characteristics of a medium. In the next stage of development the authors are extending this technique to two dimensions which will allow for model–data comparisons with realistic dispersive media, i.e. mammalian tissue.

References

[1] D.T. Blackstock, Generalized Burgers equation for plane waves, *Journal of the Acoustic Society of America* 77 (1985) 2050–2053.
[2] T.L. Szabo, Time domain nonlinear wave equations for lossy media, *Proceedings of the 13th International Symposium on Nonlinear Acoustics*, Bergen, June 1993, pp. 89–94.
[3] T.L. Szabo, Time domain wave equations for lossy media obeying a frequency power law, *Journal of the Acoustic Society of America* 96 (1994) 491–500.
[4] T.L. Szabo, Causal theories and data for acoustic attenuation obeying a frequency power law, *Journal of the Acoustic Society of America* 97 (1995) 14–24.
[5] T.L. Szabo, J. Wu, A model for longitudinal and shear wave propagation in viscoelastic media, *Journal of the Acoustic Society of America* 107 (2000) 2437–2446.
[6] R.D.L. Krönig, On the theory of dispersion of X-rays, *Journal of the Optical Society of America* 12 (1926) 547–557.
[7] K.R. Waters, M.S. Hughes, G.H. Brandenburger, J.G. Miller, On a time-domain representation of the Kramers–Krönig dispersion relations, *Journal of the Acoustic Society of America* 108 (2000) 2114–2119.
[8] G.V. Norton, J.C. Novarini, Including dispersion and attenuation directly in the time domain for wave propagation in isotropic media, *Journal of the Acoustic Society of America* 113 (2003) 3024–3031.
[9] G.V. Norton, J.C. Novarini, Including dispersion and attenuation in time domain modeling of pulse propagation in spatially-varying media, *Journal of Computational Acoustics* 12 (2004) 501–519.
[10] G.V. Norton, J.C. Novarini, Time domain modeling of pulse propagation in non-isotropic dispersive media, *Mathematics and Computers in Simulation* 69 (2005) 467–476.
[11] G.V. Norton, J.C. Novarini, Finite-difference time-domain simulation of acoustic propagation in dispersive medium: an application to bubble clouds in the ocean, *Computer Physics Communications* 174 (2006) 961–965.
[12] G.V. Norton, J.C. Novarini, Modeling ultrasonic transient scattering from biological tissues including their dispersive properties directly in the time domain, *Molecular and Cellular Biomechanics* 4 (2007) 75–85.
[13] G.V. Norton, Finite-difference time-domain simulation of acoustic propagation in heterogeneous dispersive medium, *Numerical Methods for Partial Differential Equations* 23 (2007) 1420–1428.

[14] G.V. Norton, Comparison of homogeneous and heterogeneous modeling of transient scattering from dispersive media directly in the time domain, *Mathematics and Computers in Simulation*, accepted for publication.
[15] P.M. Jordan, C.I. Christov, A simple finite difference scheme for modeling the finite-time blow-up of acoustic acceleration waves, *Journal of Sound and Vibration* 281 (2005) 1207–1216.
[16] M.F. Hamilton, C.L. Morfey, Model equations, in: M.F. Hamilton, D.T. Blackstock (Eds.), *Nonlinear Acoustics*, Academic Press, New York, 1997, pp. 41–63.
[17] R.N. Bracewell, *The Fourier Transform and its Applications*, second ed., McGraw-Hill, New York, 1986, pp. 57–61.
[18] G. Cohen, *Higher-Order Numerical Methods for Transient Wave Equations*, Springer, Berlin, 2001, pp. 45–50.
[19] J.B. Schneider, O.M. Ramahi, The complementary operators method applied to acoustic finite-difference time-domain simulations, *Journal of the Acoustic Society of America* 104 (1998) 686–693.
[20] J.P. Berenger, A perfectly matched layer for the absorption of electromagnetic waves, *Journal of Computational Physics* 114 (1994) 185–200.
[21] R.L. Higdon, Absorbing boundary conditions for difference approximations to the multi-dimensional wave equation, *Mathematics of Computation* 47 (1986) 437–459.
[22] A.D. Pierce, *Acoustics. An Introduction to its Physical Principles and Applications*, Acoustical Society of America, New York, 1989, pp. 566–617.